

REGULATION OF C-C CHEMOKINE RECEPTOR 7 (CCR7) LIGAND-MEDIATED  
INTERNALIZATION AND CHEMOTAXIS BY G PROTEIN-COUPLED  
RECEPTOR KINASE FAMILY 4 (GRK-4, 5, 6) IN HUMAN  
PEDIATRIC T-CELL ACUTE LYMPHOBLASTIC  
LEUKEMIA (T-ALL)

EDUARDO ELIAS CHAIB LOZANO

MASTER'S PROGRAM IN PUBLIC HEALTH

APPROVED:

---

Charlotte M. Vines, Ph. D. Chair

---

Gabriel Ibarra-Mejia, MD. Ph. D. Co-Chair

---

Ximena Burgos, Ph. D.

---

Colin A. Bill, Ph. D.

---

Stephen Crites, Ph. D.  
Dean of Graduate School

COPYRIGHT

By

Eduardo Elias Chaib Lozano

2022

REGULATION OF C-C CHEMOKINE RECEPTOR 7 (CCR7) LIGAND-MEDIATED  
INTERNALIZATION AND CHEMOTAXIS BY G PROTEIN-COUPLED  
RECEPTOR KINASE FAMILY 4 (GRK-4, 5, 6) IN HUMAN  
PEDIATRIC T-CELL ACUTE LYMPHOBLASTIC  
LEUKEMIA (T-ALL)

by

EDUARDO ELIAS CHAIB LOZANO, B.S.

THESIS

Presented to the Faculty of the Graduate School of

The University of Texas at El Paso

in Partial Fulfillment

of the Requirements

for the Degree of

MASTER OF PUBLIC HEALTH

Department of Public Health Sciences

The University of Texas at El Paso

May 2022

## **ACKNOWLEDGEMENTS**

I want to express my deep gratitude for the opportunity to join Dr. Charlotte Vines' and Dr. Colin Bill's laboratory. They made this project possible and always encouraged me to keep on going. I also want to thank my committee members Dr. Gabriel Ibarra and Dr. Ximena Burgos, who were always supportive and encouraged me to improve myself. I want to thank Dr. Nadine Gehre who guided me in the initial portions of my research. And lastly, I want to thank every professor and student in The University of Texas at El Paso's BioScience Building who taught me something along this process, I sincerely appreciate all your patience and generous attitude.

## ABSTRACT

**Background and Significance:** The Hispanic population is disproportionately affected by T-ALL (T-cell acute lymphoblastic leukemia) when compared to other races in the US. C-C Chemokine Receptor 7 (CCR7) in T-ALL is used during disease progression, and may lead to migration of cancerous cells into the Central Nervous System (CNS) of patients. **Goals and Objectives:** This project aims to find relevant rates and risk factors for T-ALL for the Hispanic population in the US/Mexico border region. The other aim is to assess the effect of the G protein-coupled Receptor Kinase 4 (GRK-4) family proteins on migration and receptor internalization through CCR7 in T-ALL. **Hypothesis:** The inactivation of the GRK-4 family genes (specifically GRK-5 and -6) in cancerous cells (CEM and Hut-78) will produce a reduction in CCR7-directed migration of these T-ALL cells towards the CCR7 ligands CCL19 and/or CCL21. **Methods:** Local, state, and national health data agencies were queried for relevant rates of, and data about T-ALL in Hispanics living in the US/Mexico border region. GRK-5, and -6 genes were individually targeted using CRISPR-Cas9 in T-ALL cells to inhibit protein expression. **Results:** Data about T-ALL in the border region and the city of El Paso is scarce and has discrepancies among different agencies. Leukemias are the most common cancers in children 0 to 20 years of age, and the Hispanic population is more heavily affected than the non-Hispanic White population according to some sources. The expression of GRKs was not reduced with the CRISPR lentivirus approach, but it was somewhat reduced through esiRNA nucleofection. **Conclusions:** T-ALL is tied to several environmental factors and living conditions that apply to the Hispanic population in the US/Mexico region. Preventing the incidence of this disease requires health awareness interventions and safety regulations in industries where workers are exposed to, or handle leukemogens. The CRISPR-Cas9 experimental results showed no

reduction in the expression of GRK-5 or -6, but GRK-6 was partially reduced after esiRNA nucleofection, which could provide an alternative to test the chemotactic and internalization properties of cells once these kinases are inhibited.

PREVIEW

## TABLE OF CONTENTS

ACKNOWLEDGEMENTS.....	iv
ABSTRACT.....	v
TABLE OF CONTENTS.....	vi
TABLE OF FIGURES.....	vii
CHAPTER 1: LITERATURE REVIEW.....	1
BACKGROUND.....	1
INTRODUCTION.....	7
PROBLEM STATEMENT.....	17
SIGNIFICANCE.....	21
GOALS AND OBJECTIVES .....	23
HYPOTHESIS.....	23
CHAPTER 2: METHODS .....	24
CHAPTER 3: TIMELINE .....	33
CHAPTER 4: RESULTS AND DISCUSSION.....	34
RESULTS.....	34
DISCUSSION.....	54
GAPS IN LITERATURE.....	55
CONCLUSION.....	60
CHAPTER 5: MPH CORE COMPETENCIES.....	61
CHAPTER 6: HEALTHY PEOPLE 2020 OBJECTIVES.....	62
CHAPTER 7: HISPANIC/BORDER HEALTH CONCENTRATION COMPETENCIES.....	64

REFERENCES.....	68
CURRICULUM VITA .....	78

PREVIEW



## TABLE OF FIGURES

Figure 1. Age-adjusted incidence rate for Hispanic and non-Hispanic children from 1992-2011 in the United States. (Barrington-Trimis, 2015). .....	2
Figure 2. Age-Adjusted Invasive Cancer incidence rates in Texas by county (2012-2016). (Texas Cancer Registry, 2019).....	4
Figure 3. General GPCR ligand-mediated recycling and degradation pathways in a cellular membrane (Zhukovskaya, 2013). .....	8
Figure 4. G-protein $\alpha\beta\gamma$ subunits and some of their downstream signaling cascades (Heldin, 2016).....	9
Figure 5. GRK genetic domains among the GRKs subtypes (Gurevich, 2012).....	12
Figure 6. Migration of T-cells to chemokine gradients of CCL19 and CCL21 in HEVs of a lymph node (Comerford, 2013). .....	13
Figure 7. G- $\alpha$ proteins activated by CCL19 and CCL21 through CCR7 and their downstream effects (Jorgensen, 2018).....	14
Figure 8. CRISPR-directed K.O. mechanism for protein inhibition (Ebner, 2019).....	22
Figure 9. Hispanic local, state, and national rates associated with T-ALL from different health agencies. (*): Areas in the US with "High" quality incidence data. (-): No data available. (**): SEER includes data on 9 specific states/regions of the country.....	34
Figure 10. Flow cytometry of CEM cells membrane to detect CCR7 (blue and orange peaks), isotype control (green peak), and untreated cells (red peak).....	36
Figure 11. Flow cytometry of HuT-78 cells membrane to detect CCR7 (blue and orange peaks), isotype control (green peak), and untreated cells (red peak).....	36
Figure 12. Western blot of CEM and HuT-78 cells after inoculation with each separate CRISPR lentivirus and probed with an GRK-4-6 antibody (65-70 kDa). Sample order from left to right: (a: control CEM, b: CRISPR GRK-4 CEM, c: CRISPR GRK-5 CEM, d: CRISPR GRK-6 CEM, e: control HuT-78, f: CRISPR GRK-4 HuT-78, g: CRISPR GRK-5 HuT-78, h: CRISPR GRK-6 HuT-78).....	39

Figure 13. Western blot of CEM (control, CRISPR GRK-4, -5, and -6) and HuT-78 (control, CRISPR GRK-4, -5, and -6) cells after inoculation with each separate GRK-CRISPR lentivirus and probed with a GRK-5 antibody (68 kDa). Sample order from left to right: (a: control CEM, b: CRISPR GRK-4 CEM, c: CRISPR GRK-5 CEM, d: CRISPR GRK-6 CEM, e: control HuT-78, f: CRISPR GRK-4 HuT-78, g: CRISPR GRK-5 HuT-78, h: CRISPR GRK-6 HuT-78).....	39
Figure 14. Western blot of CEM control cells and CEM-CRISPR-GRK-6 treated cells with a GRK-6 antibody probe (66 kDa). Sample order from left to right: (L: ladder, a: control CEM, b: CRISPR GRK-6 CEM).....	40
Figure 15. A) Non-treated HuT-78 cells without PI observed in a flow cytometer before nucleofection (99.40 % live cells). B) Non-treated HuT-78 cells with PI observed in a flow cytometer before nucleofection (94.04 % live cells).....	41
Figure 16. HuT-78 cells 72-hours after nucleofection (no DNA plasmid added), observed in a flow-cytometer (18.99 % live cells).....	41
Figure 17. A) HuT-78 cells 72 hours after nucleofection (2 µg of DNA plasmid were added to 1 million cells), observed in a flow-cytometer (41.90 % live cells). B) HuT-78 cells 72 hours after nucleofection (4 µg of DNA plasmid were added to 1 million cells), observed in a flow-cytometer (56.51 % live cells).....	42
Figure 18. Non-nucleofected HuT-78 control cells viewed under a light microscope 10x.....	42
Figure 19. One million HuT-78 cells 72 hours after nucleofection with 4 µg of GFP plasmid viewed under a light microscope (10x).....	43
Figure 20. One million HuT-78 cells 72 hours after nucleofection with 2 µg of GFP plasmid viewed under a light microscope (10x).....	43
Figure 21. CEM cells inoculated with 100 µl of pCDH-EF1-Luc2-P2A-tdTomato lentivirus, seen after 72 hours post inoculation viewed under a light microscope at 20x.....	44
Figure 22. CEM cells inoculated with 400 µl of pCDH-EF1-Luc2-P2A-tdTomato lentivirus, seen after 72 hours post inoculation viewed under a light microscope at 20x.....	44

Figure 23. A) CEM cells without PI before nucleofection (99.56 % live cells). B) CEM with PI before nucleofection (97.43 % live cells).....	45
Figure 24. A) HuT-78 cells without PI before nucleofection (99.69 % live cells). B) HuT-78 with PI before nucleofection (93.13 % live cells).....	45
Figure 25. A) CEM control cells (2 million) 48 hours post nucleofection without esiRNA (6.92 % live cells). B) HuT-78 control cells (2 million) 48 hours post nucleofection without esiRNA (72.62 % live cells).....	46
Figure 26. A) 1 million CEM cells 48 hours post nucleofection using 1 µg esiRNA (4.33 % live cells). B) 1 million HuT-78 cells 48 hours post nucleofection using 1 µg esiRNA (58.73 % live cells). ....	46
Figure 27. A) 2 million CEM cells 48 hours post nucleofection using 2 µg esiRNA (15.26 % live cells). B) 2 million HuT-78 cells 48 hours post nucleofection using 2 µg esiRNA (32.06 % live cells).....	47
Figure 28. A) 3 million CEM cells 48 hours post nucleofection using 3 µg esiRNA (3.88 % live cells). B) 3 million HuT-78 cells 48 hours post nucleofection using 3 µg esiRNA (39.17 % live cells).....	47
Figure 29. A). Western blot of CEM cells treated with esiRNA-GRK-6 and using a GRK-6 antibody (66kDa). Sample order from left to right: a: CEM control, b: CEM 72h 3:3, c: CEM 72h 2:2, d: CEM 72h 1:1, e: CEM nucleop. w/o esiRNA, f: CEM 48h 3:3, g: CEM 48h 2:2, h: CEM 48h 1:1, L: ladder. B) Western blot membrane after stripping and re-probing for β-actin (45kDa).....	48
Figure 30. Densitometry quantification of GRK-6 expression Western blot after esiRNA nucleofection of CEM cells. Results normalized to housekeeping gene expression. Thermo Fisher Scientific iBright IBA online platform was used for densitometry.....	48
Figure 31. A). Western blot of CEM cells treated with esiRNA-GRK-6 and using a GRK-6 antibody (66kDa). Sample order from left to right: a: CEM control, b: CEM 72h 3:3, c: CEM 72h 2:2, d: CEM nucleop. w/o esiRNA, e: CEM 48h 3:3, f: CEM 48h 2:2, L: ladder. B) Western blot membrane after stripping and re-probing for β-actin (45kDa).....	49
Figure 32. Densitometry quantification of GRK-6 expression Western blot after esiRNA nucleofection of CEM cells. Results normalized to housekeeping gene expression. Thermo Fisher Scientific iBright IBA online platform was used for densitometry.....	49

Figure 33. A). Western blot of HuT-78 cells treated with esiRNA-GRK-6 and using a GRK-6 antibody (66kDa). Sample order from left to right: L: ladder, a: HuT-78 48h 1:1, b: HuT-78 48h 2:2, c: HuT-78 48h 3:3, d: HuT-78 nucleop. w/o esiRNA, e: HuT-78 72h 1:1, f: HuT-78 72h 2:2, g: HuT-78 72h 3:3, h: HuT-78 control. B) Western blot membrane after stripping and re-probing for GAPDH (37kDa).....50

Figure 34. Densitometry quantification of GRK-6 expression Western blot after esiRNA nucleofection of HuT-78 cells. Results normalized to housekeeping gene expression. Thermo Fisher Scientific iBright IBA online platform was used for densitometry.....50

Figure 35. A). Western blot of HuT-78 cells treated with esiRNA-GRK-6 and using a GRK-6 antibody (66kDa). Sample order from left to right: L: ladder, a: HuT-78 48h 1:1, b: HuT-78 48h 2:2, c: HuT-78 48h 3:3, d: HuT-78 nucleop. w/o esiRNA, e: HuT-78 72h 1:1, f: HuT-78 72h 2:2, g: HuT-78 72h 3:3, h: HuT-78 control. B) Western blot membrane after stripping and re-probing for GAPDH (37kDa).....51

Figure 36. Densitometry quantification of GRK-6 expression Western blot after esiRNA nucleofection of HuT-78 cells. Results normalized to housekeeping gene expression. Thermo Fisher Scientific iBright IBA online platform was used for densitometry.....51

Figure 37. Infiltration of cancerous cells into leptomeninges and adaptation of the CSF composition through blood-brain barrier disorganization (Boire, 2017).....57

Figure 38. Annual age-adjusted rates per 1,000,000 people for ALL who are younger than 20 years of age in the United States from 2001-2014 (Siegel, 2017).....66

## **CHAPTER 1: LITERATURE REVIEW BACKGROUND**

The city of El Paso, Texas is located along the United States-Mexico border and its population is predominantly of Hispanic descent (82.8%) (US Census Bureau, 2017). The Hispanic population has been documented to be disproportionately affected by diseases such as diabetes, cardiovascular disease, and several types of cancers when compared to other races in the United States (Rodriguez, 2014; Aviles-Santa, 2017; Center for Disease Control and Prevention, 2017). Epidemiological data shows that cancer incidence and mortality rates have increased over the last decades for all races in the country (Barrington-Trimis, 2015, American Cancer Society, 2018), however, there has been a significant increase in the incidence of Acute Lymphoblastic Leukemias (ALLs) within the Hispanic population at younger ages (<20 years of age) when compared to other non-Hispanic individuals (Darbinyan, 2008; Barrington-Trimis, 2015 Bencomo-Alvarez, 2020). Some factors like living conditions, socio-economic levels, education, health awareness, risk behaviors, culture, nutrition, pathology, genetics, and other variables are known to influence the risk perception, incidence, progression, and treatment of different forms of cancers for different populations (Aviles-Santa, 2017; Siegel, 2017).

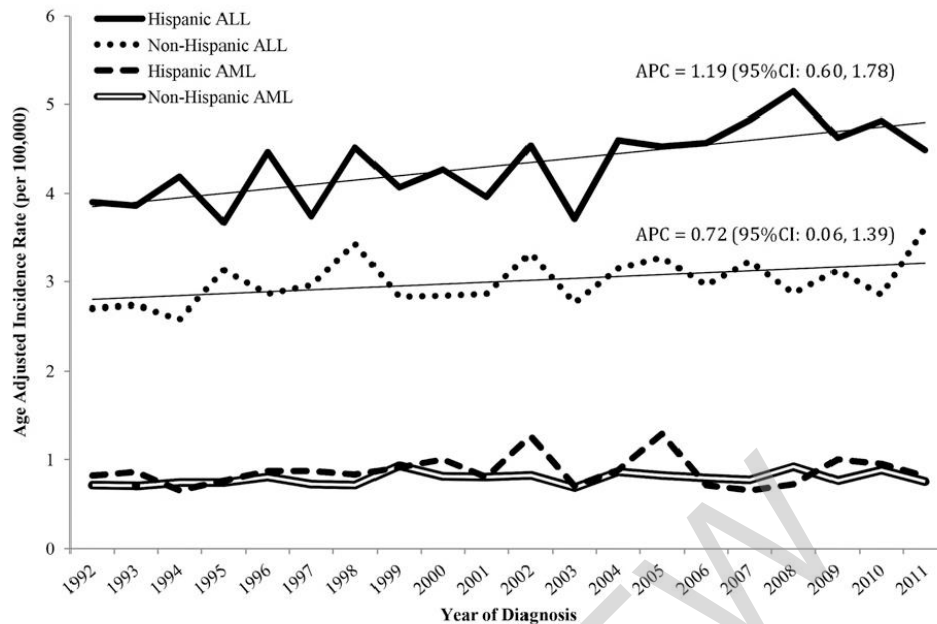


Figure 1. Age-adjusted incidence rate for Hispanic and non-Hispanic children from 1992-2011 in the United States. (Barrington-Trimis, 2015)

The Texas Cancer Incidence Reporting Act requires local hospitals, clinical laboratories, and physician practices to report cancer cases according to the Texas Health and Safety Code Section 82.007, but reporting requirements vary depending on the facility (Texas Department of State Health Services, 2019; 2020). Some of the agencies that collect relevant health data are: The Healthy Paso del Norte Foundation, the Texas Department of State Health Services, the Texas Cancer Institute, and the Healthy People 2020 organization. These agencies have recorded data at the local, state, and national levels, and they are updated as the years pass or as progress is made on specific organizational objectives. To date, there are few registries with current and comprehensive information about ALLs, and there is a specific lack of data on studies about T-cell ALL (T-ALL) in large pediatric groups (Fuhrman, 2018). The Surveillance, Epidemiology, and End Results Program (SEER) database was created by the National Cancer Institute, and it is considered the “gold standard” for population-based research, despite a few caveats (Howlader,

2020; Kinslow, 2020). SEER is based on the insurance claims of some specific regions and states in the country (Texas is not included), which means that it may not accurately represent all populations in the United States. Another consideration is that its data has differences with the other previously mentioned sources of health data. These differences, and the lack of data collection in some regions/states could be underrepresenting the severity of ALLs for the different population groups in the country. This suggests the need for public health interventions and preventive screening services, but there are specific problems in the border region that further complicate these efforts. The US-Mexico border is one of the busiest in the world, and it has had increasing problems with illegal immigration and other related regional issues (Healthy Border 2020, 2015). Illegal immigration status, the fear of deportation, the lack of insurance, lower socioeconomic status, language barriers, and access to care have been documented as the basis for the lack of people seeking medical attention and/or participating in health programs (Bickell, 2008; American Cancer Society, 2018; Healthy Border 2020, 2015; Bencomo-Alvarez, 2020). These local issues require more extensive planning, prevent the proper utilization of health programs, and ultimately affect intervention efforts in the region.

Age-Adjusted Invasive Cancer Incidence Rates in Texas  
 Acute Lymphocytic Leukemia, Hispanic, 2012 - 2016  
 By County  
 Age-Adjusted to the 2000 U.S. Standard Population

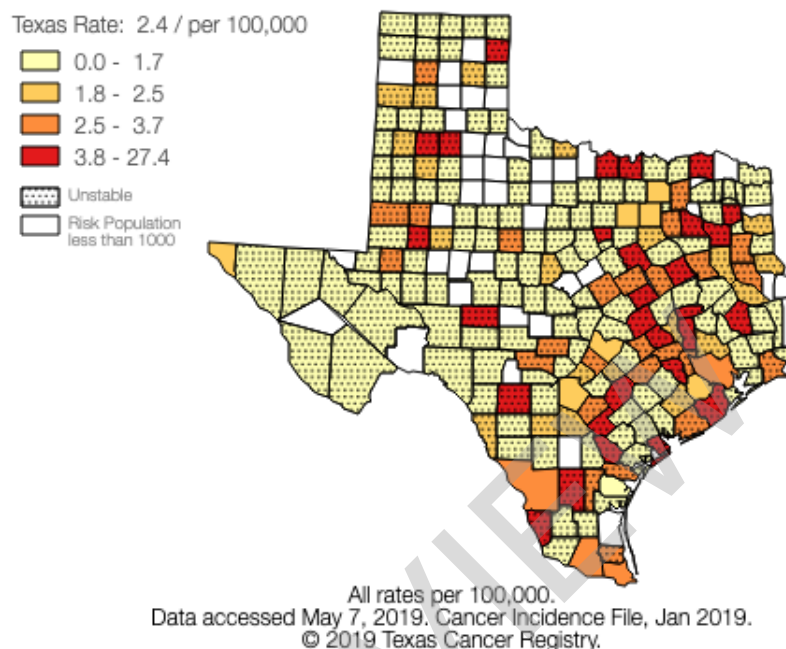


Figure 2. Age-Adjusted Invasive Cancer incidence rates in Texas by county (2012-2016). (Texas Cancer Registry, 2019).

There are many factors that influence the incidence and prevalence of cancer, among them there are inherent factors which cannot be controlled like genetic predispositions, ethnicity, gender, and age. However, there are other factors such as risk behaviors, nutrition, health awareness, and to some degree socioeconomics, education, and the environment, which can be modified to improve the health and quality of life of a population (American Cancer Society, 2018; Aviles-Santa, 2017; Siegel, 2017). Public health programs and interventions can help initiate these improvements, but they require comprehensive research and needs assessments to identify the current health problems in a region and populations of interest. These studies can help identify baseline measures, and barriers that should be considered when designing an intervention program for a given community. The collection of data about ALL's would allow the city of El Paso to create disease registries that accurately document the local burden of



disease and help identify the risks factors that may be predisposing this population to develop these types of cancers. Collecting local population-based data would also be a good way to identify treatment-related outcomes (Kinslow, 2020) and could also help promote awareness of risk factors in the region.

Healthcare interventions can be reinforced by involving both the healthcare providers and the patients/community for the improvement of health conditions. Introducing cultural competence, improving health literacy, and increasing access to health programs can reduce health disparities by making patients feel more comfortable and willing to follow medical advice (Kagawa-Singer, 2010; Rodriguez, 2014; Winestone, 2019). Preventive practices, health awareness, and screening programs could be enhanced through collaboration between community leaders, medical ethicists, and activists who are actively engaged within their communities. These joint efforts would be effective in educating the general public by integrating patients and local community leaders in the promotion of healthier lifestyles and safer behaviors for their communities (Rodriguez, 2014; ACS, 2018). These approaches reinforce the communication between patients and doctors, encourage proper consultation of medical advice, reduce barriers to medical treatment (and increases adherence to it), and ultimately reduce health disparities among the population (Bickell 2008; Winestone, 2019). The combined data collected from researchers, data registries, public health professionals, physicians, community activists, and patients could be used to develop more complete strategies to promote health awareness and preventive screening for ALLs.

The mechanisms of cancer development and progression have been extensively investigated and are continuously updated to map the specific cellular pathways that generate and sustain malignancies. Different types of cancers are induced by distinct genetic mutations

and/or dysregulated cellular processes, which ultimately alter the homeostatic physiological functions of cells. The accumulation of these genetic mutations converts cells into a malignant state by activating oncogenes, deactivating tumor suppressor genes, and dysregulating cellular growth patterns that can ultimately become tumors/malignancies with additional health consequences (Grabher, 2006; O'Hayre, 2014; Korbecki, 2020). The technical details about the specific mechanisms that promote T-ALL progression may be of little significance to the lay population of El Paso, but a more thorough understanding of the etiology of the disease can help improve current treatment options, which would ultimately improve survival rates, and increase public health awareness and education in the El Paso/Juarez region and other border communities. This project aims to define the function of some mediators of T-ALL signaling pathways, specifically the G-Protein Coupled Receptor (GPCR) C-C Chemokine Receptor type 7 (CCR7). This pathway is important for T-ALL progression because CCR7 expression has been consistently observed in tissue samples from patients with this disease (Buonamici, 2009; Korbecki, 2020).

## INTRODUCTION

GPCRs are the largest family of cell-surface receptors (>800) in humans that modulate many physiological functions (neurotransmission, cardiac activity, blood pressure, homeostasis, metabolism, sensory perception, immune response, and growth processes, among others) in virtually all cells. GPCRs are expressed in species ranging from *Homo sapiens* to Metazoans (animal) (Premont, 2007; Zhukovskaya, 2013; Heldin, 2016; Korbecki, 2020). Signaling through GPCRs is just one type of signaling system used by cells to adapt to their environment, however, there are other signaling systems through other types of receptors and channels in cells (Heldin, 2016). The general structure of GPCRs consist of 7 transmembrane  $\alpha$ -helices which span the extracellular and intracellular faces of a cell membrane. Once a GPCR binds to an extracellular ligand, a conformational change is triggered in the intracellular face of the  $\alpha$ -helices of the GPCR and the C-terminus becomes a “Guanosine Exchange Factor” (GEF). This “GEF” regulates exchange of guanosine triphosphate (GTP) on the associated G-proteins, which are an assembly of 3 different (heterotrimeric) subunits (Zhou, 2017). There are G-protein alpha ( $G\alpha$ ), beta ( $G\beta$ ), and gamma ( $G\gamma$ ) subunits, and each of them has several genetic variants (Premont 2007; Syrovatkina, 2016). To date, 16 to 21  $G\alpha$  isoforms (organism specific), 6  $G\beta$  isoforms, and 12  $G\gamma$  isoforms have been identified, although new ones continue to be described (Minh Duc, 2015; Zhou 2017). When the G-proteins are in their “inactive” state, the 3 subunits are bound in the heterotrimeric ( $G\alpha$ ,  $\beta/\gamma$ ) conformation. While in this inactive state, the G-alpha ( $G\alpha$ ) subunit is bound to a guanosine-5'- diphosphate molecule ( $G\alpha$ -GDP), and the G-beta-gamma ( $G\beta/\gamma$ ) subunits are almost always bound to each other and are considered a joint functional unit. This allows for many possible combinations of G-protein subunit complexes, which can interact with